Journal of Molecular Structure 933 (2009) 148–155

Contents lists available at ScienceDirect

Journal of Molecular Structure

journal homepage: www.elsevier.com/locate/molstruc

X-ray structural characterizations of the reaction products between $ZnCl_2$ and 6-benzylaminopurine derivatives in different acidic conditions

Zdeněk Trávníček [a,*], Jaromír Marek [a,b]

[a] Department of Inorganic Chemistry, Faculty of Science, Palacký University, Křížkovského 10, CZ-771 47 Olomouc, Czech Republic
[b] Institute of Experimental Biology, Faculty of Science, Masaryk University, CZ-625 00 Brno, Czech Republic

ARTICLE INFO

Article history:
Received 14 January 2009
Received in revised form 5 June 2009
Accepted 5 June 2009
Available online 13 June 2009

Keywords:
Zinc(II) complexes
Tautomerism
Protonation
6-Benzylaminopurine
Crystal structures

ABSTRACT

The reaction between $ZnCl_2$ and the corresponding 6-benzylaminopurine derivative, L_n, [where L_1 = 6-(4-fluorobenzylamino)purine, L_2 = 6-(2-fluorobenzylamino)purine or L_3 = 6-(4-chlorobenzylamino)purine] in 0.1 M or 2 M HCl afforded various products in dependence on a pH of the reaction medium. X-ray structures of the reaction products have been determined by a single crystal X-ray analysis. It has been found that the reaction led to the formation of $[Zn(HL_1)Cl_3]\cdot H_2O$ (**1**) in 0.1 M HCl in which the L_1 ligand acts as the single N1–H protonated N9–H tautomer and is coordinated to Zn through N7 atom of a purine skeleton. On the other hand, ion-paired compounds of the composition $(H_2L_2)[ZnCl_4]\cdot H_2O$ (**2**) and $(H_2L_3)[ZnCl_4]$ (**3**) have been formed during the reactions in 2 M HCl. Each of the organic molecules L_2 and L_3 is twice protonated and its positive charge is compensated by the presence of the $[ZnCl_4]^{2-}$ anion. The cation exists as the N1–H, N7–H protonated N9–H tautomer in (**2**), and as the N3–H, N7–H protonated N9–H one in (**3**). It has been found that the extent of protonation has a significant impact on the coordination ability of the discussed organic molecules, and as a result of this finding, also on selected interatomic parameters as well as non-bonding interactions present in their crystal structures. Moreover, the compounds have been characterized by elemental analyses (C, H, N), FTIR and Raman spectroscopies, and thermogravimetric (TG) and differential thermal (DTA) analyses.

1. Introduction

The organic compounds bearing the 6-benzylaminopurine (Bap) moiety, belonging to a group of plant growth hormones, called cytokinins (CKs), have been studied since the 1960s. The CKs represent a group of compounds, which can significantly affect some of physiological functions, e.g. plant cell divisions, senescence, etc. [1,2]. Moreover, the substitution of the Bap skeleton at the C2 and N9 positions by suitable side chains may lead to the formation of compounds having the ability to behave as cyclin-dependent kinase inhibitors (CDKIs). The cyclin-dependent kinases belong to the family of protein kinases responsible for the regulation of the cell cycle [3]. Moreover, some of the CDKIs involving the Bap moiety demonstrate considerable both *in vitro* and *in vivo* cytotoxicity against some human cancer cell lines [4]. Based on our previously published results, we have found that the cytotoxicity may be increased after the coordination of both CKs and CDKIs to suitable transition metal ions [5,6]. Moreover, it may be concluded that the coordination ability of Bap derivatives strongly depends on an extent of substitution of the Bap skeleton and reaction conditions used during the synthesis such as a medium pH, the molar ratio of reactants, and solvents used.

To date, 22 molecular structures of Zn(II) complexes involving adenine moiety have been deposited within the Cambridge Structural Database (CSD ver. 5.29, August 2008 update) [7]. One of three presented X-ray structures of Zn(II) compounds, i.e. complex (**1**), represents the first example of a Zn(II) complex containing the aromatic CKs derived from the Bap skeleton, except for those involving the CDKIs derived from the same skeleton, i.e. $[Zn(Olo)Cl_2]_n$, $[Zn(HBoh)Cl_3]\cdot H_2O$ and $[Zn(HiprOlo)Cl_3]\cdot H_2O$ [8], where Olo = 2-(2-hydroxyethylamino)-6-benzylamino-9-methylpurine (Olomoucine), Boh = 2-(3-hydroxypropylamino)-6-benzylamino-9-isopropylpurine (Bohemine), *ipr*Olo = 2-(2-hydroxyethylamino)-6-benzylamino-9-isopropylpurine (*iso*propyl-Olomoucine). Both the $[Zn(HBoh)Cl_3]\cdot H_2O$ and $[Zn(HiprOlo)Cl_3]\cdot H_2O$ mentioned complexes have been found to be significant inhibitors of the CDK2/cyclin E kinase with IC_{50} = 0.40 and 0.50 μM, respectively [8].

Herein, the syntheses and X-ray structures of one Zn(II) complex (**1**) and two Zn(II) ion-paired compounds (**2**) and (**3**) involving the selected Bap derivatives are presented. One of the motivations of this study was to make attempts and to find how the composition of the reaction products can be influenced by a degree of acidity of the reaction medium used during the synthesis.

* Corresponding author. Tel.: +420 585634944; fax: +420 585634954.
E-mail address: zdenek.travnicek@upol.cz (Z. Trávníček).

0022-2860/$ - see front matter © 2009 Elsevier B.V. All rights reserved.
doi:10.1016/j.molstruc.2009.06.011

2. Experimental

2.1. Materials and general methods

$ZnCl_2 \cdot 1.5H_2O$ was used as received from Sigma–Aldrich Co. 6-(4-Fluorobenzylamino)purine (L_1), 6-(2-fluorobenzylamino) purine (L_2) and 6-(4-chlorobenzylamino)purine (L_3), used as ligands in this study, were prepared by the method described in the literature [9]. Elemental analyses (C, H, N) were performed on a Flash EA–1112 Elemental Analyser (Thermo Finnigan). Determinations of the melting points were performed using a Melting Point B-540 apparatus (Büchi) with the gradient of 5 °C per minute and were uncorrected. Infrared spectra were obtained on a Nexus 670 FTIR spectrometer (Thermo Nicolet) using KBr (4000–400 cm^{-1}) and ATR (600–200 cm^{-1}) techniques. Raman spectra were recorded on a NXR FT–Raman Module (ThermoNicolet) in the range of 150–3750 cm^{-1}. Simultaneous thermogravimetric (TG) and differential thermal (DTA) analyses were carried out using a thermal analyzer Exstar TG/DTA 6200 (Seiko Instruments Inc.) with sample weights of about 10 mg. TG/DTA studies were performed in ceramic pans between the laboratory temperature and 800 °C with a 5 °C min^{-1} temperature gradient in dynamic air atmosphere (150 mL min^{-1}).

2.2. X-ray crystallography

Diffraction data for single crystals of complexes (**1**), (**2**) and (**3**) were collected at 100 K on an Xcalibur2 diffractometer (Oxford Diffraction, Ltd.) with Mo K_α (monochromator Enhance, Oxford Diffraction, Ltd.) radiation and ω-scan rotation techniques. The data were reduced using the *CrysAlis* software package (Oxford Diffraction, Ltd.) [10]. A multi-scan absorption correction integrated in the *CrysAlis* software was applied on the data of all three compounds. All three structures were determined by direct methods using SHELXS-97 and refined anisotropically on F^2 using a full-matrix least-squares procedure by SHELXL-97 [11] with weight: $w = 1/[\sigma^2(F_o)^2 + (0.035P)^2 + 1.500P]$ for (**1**), $w = 1/[\sigma^2(F_o)^2 + (0.025P)^2 + 1.500P]$ for (**2**) and $w = 1/[\sigma^2(F_o)^2 + (0.035P)^2 + 1.500P]$ for (**3**), where $P = (F_o^2 + 2F_c^2)/3$. All H-atoms were found from Fourier maps and refined with a riding model, with C—H distances of 0.95–0.99 Å and N—H distances of 0.88 Å, and with U_{iso}(H) values of 1.2 U_{eq} C,N. The H-atoms of water molecules of crystallization were refined with the O—H distances restrained to 0.95(2) Å. All structural figures were made with DIAMOND [12].

2.3. Synthesis of the complexes

2.3.1. Synthesis of $[Zn(HL_1)Cl_3]\cdot H_2O$ (**1**)

The complex was prepared by mixing of equimolar solutions of $ZnCl_2 \cdot 1.5H_2O$ (1 mmol) and the L_1 ligand (1 mmol) in 30 ml of 0.1 M HCl. The reaction mixture was stirred and heated at 80 °C for 4 h. The resulting solution was kept at room temperature for several days. Colourless crystals of (**1**), suitable for a single crystal X-ray analysis, were obtained by slow evaporation of the solvent from the reaction solution. As for the FTIR, Raman and TG/DTA studies, the complex was prepared by the same procedure in the form of $[Zn(HL_1)Cl_3]\cdot(HL_1Cl)\cdot MeOH$ (**1a**).

For (**1**). Yield: 73%. Anal. Calcd. for $C_{12}H_{11}Cl_3FN_5Zn\cdot H_2O$ (M_r = 434.0): C, 33.2; H, 3.0; N, 16.1%. Found: C, 33.1; H, 3.0; N, 15.9%.

For (**1a**). Yield: 80%. Anal. Calcd. for $C_{12}H_{11}Cl_3FN_5Zn\cdot C_{12}H_{11}ClFN_5\cdot CH_3OH$ (M_r = 727.7): C, 41.3; H, 3.6; N, 19.2%. Found: C, 40.9; H, 3.9; N, 18.9%. IR (ATR; cm^{-1}): 576vs, 551m, 535s, 518s, 485s, 432m, 419m, 329s, 288vs, 209w. IR (KBr; cm^{-1}): 3422w, 3274w, 3121w, 3066w, 2971w, 1656vs, 1606s, 1510s, 1447w, 1432w, 1403m, 1349m, 1295m, 1223s, 1159m, 1126w, 1097w, 1041w, 1015w, 971w, 825m, 793w, 779w, 765w, 637w, 610m, 577w, 532w. Raman (cm^{-1}): 3285w, 3198w, 3114w, 3071s, 3006w, 2946m, 1605s, 1508s, 1471w, 1402s, 1344s, 1291m, 1222m, 1157m, 1121m, 970m, 853s, 827m, 734s, 638m, 576m, 529w, 493m, 422m, 326m, 283s, 234m.

2.3.2. Synthesis of $(H_2L_2)[ZnCl_4]\cdot H_2O$ (**2**) and $(H_2L_3)[ZnCl_4]$ (**3**)

The complexes were prepared by mixing of equimolar solutions of $ZnCl_2 \cdot 1.5H_2O$ (1 mmol) and L_2, and L_3 (1 mmol), respectively, in 30 ml of 2 M HCl. The reaction mixtures were stirred and heated at 80 °C for 4 h. The resulting solutions were kept in the room temperature for 14 days. Colourless crystals, suitable for a single crystal X-ray analysis, were obtained by slow evaporation of the solvent from the reaction solutions. The schematic representation of the synthetic pathways for the preparation of the complexes (**1**)–(**3**) is depicted in Scheme 1.

For (**2**). Yield: 58%. M.p. 228–230 °C. Anal. Calcd. for $C_{12}H_{12}FN_5\cdot Cl_4Zn\cdot H_2O$ (M_r = 470.5): C, 33.2; H, 3.0; N, 16.1%. Found: C, 33.1; H, 3.0; N, 15.9%. IR (ATR; cm^{-1}): 547s, 520s, 468s, 434m, 378w, 321s, 282vs, 259vs. IR (KBr; cm^{-1}): 3443m, 3205m, 3161w, 3112m, 3072m, 2984w, 2936w, 1675vs, 1609vs, 1588s, 1522m, 1493s, 1454m, 1419s, 1353m, 1288w, 1233s, 1215s, 1182w, 1139m, 1107m, 1033m, 999m, 976m, 954w, 899m, 848m, 764vs, 734m, 656m, 635s, 565w, 546m, 521s. Raman (cm^{-1}): 3116m, 3073s, 2949m, 1687m, 1618m, 1594m, 1523w, 1474m, 1422s, 1337s, 1282vs, 1233w, 1159m, 1136w, 1109w, 1033s, 978s, 949m, 894w, 777vs, 737m, 723m, 524s, 436w, 383m, 278s, 223w.

For (**3**). Yield: 53%. M.p. 234–236 °C. Anal. Calcd. for $C_{12}H_{12}ClN_5\cdot Cl_4Zn$ (M_r = 468.9): C, 30.7; H, 2.6; N, 14.9%. Found: C, 30.5; H, 2.6; N, 15.0%. IR (ATR; cm^{-1}): 543vs, 528m, 480s, 403m, 313vs, 277vs, 253s. IR (KBr; cm^{-1}): 3446m, 3302m, 3212m, 3174w, 3129m, 1654vs, 1625s, 1568s, 1493s, 1477m, 1464s, 1440s, 1408s, 1395m, 1343s, 1263m, 1209s, 1190w, 1169m, 1121s, 1108m, 1095m, 1015s, 983m, 967w, 908w, 883w, 801s, 778w, 722vs, 637w, 610s, 544s, 527w, 481s. Raman (cm^{-1}): 3129w, 3065s, 2926m, 1656m, 1623s, 1599w, 1567w, 1512s, 1478m, 1441w, 1396m, 1373vs, 1344vs, 1263w, 1204m, 1170w, 1124vs, 1107vs, 982m, 843s, 765s, 684s, 639m, 542m, 403w, 304s, 288s, 234w.

3. Results and discussion

3.1. X-ray molecular and crystal structures

Crystallographic data and refinement details for compounds (**1**), (**2**) and (**3**) are summarized in Table 1, while the selected bond lengths and angles are given in Table 2. All important hydrogen-bonding interactions are given in Table 3.

3.1.1. Molecular and crystal structures of $[Zn(HL_1)Cl_3]\cdot H_2O$ (**1**)

The molecular structure of (**1**) together with the atom numbering scheme is shown in Fig. 1. The central Zn(II) ion is tetrahedrally coordinated by three chlorido ligands and one HL_1 molecule through the N7 atom of an adenine moiety. The Zn—Cl and Zn—N bond lengths (see Table 2) are comparable with the average bond length of 2.316(13) and 2.091(7) Å, respectively, as found in 50 compounds containing a $ZnCl_3N$ motive which are deposited in CSD [7]. As for the Zn—Cl and Zn—N distances in the complex (**1**), these are also comparable to those found in $[Zn(HBoh)Cl_3]\cdot H_2O$ and $[Zn(HiprOlo)Cl_3]\cdot H_2O$ for which Zn—Cl and Zn—N distances range from 2.2269(14) to 2.2719(14) Å, and from 2.045(4) to 2.0311(18) Å, respectively [8]. It is well known that molecules involving an adenine skeleton may behave as ligands suitable for coordination to transition metals owing to five nitrogen atoms to be present within their molecules. Based on the search within

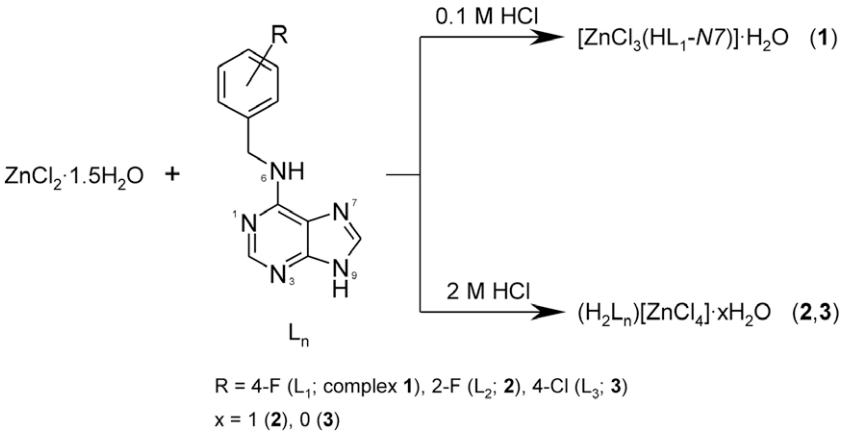

Scheme 1. A schematic representation of the synthetic pathways for the preparation of the complexes (**1**)-(**3**).

Table 1
Crystallographic data and refinements for (**1**), (**2**) and (**3**).

	(**1**)	(**2**)	(**3**)
Formula	$C_{12}H_{11}Cl_3FN_5Zn.H_2O$	$C_{12}H_{12}FN_5.Cl_4Zn.H_2O$	$C_{12}H_{12}ClN_5.Cl_4Zn$
M (g mol^{-1})	433.99	470.45	468.89
T (K)	100(2)	100(2)	100(2)
λ (Å)	0.71073	0.71073	0.71073
Crystal system	monoclinic	monoclinic	monoclinic
Space group	$P2_1/c$	$P2_1/n$	$P2_1/c$
a (Å)	8.98995(19)	9.92791(18)	18.9463(8)
b (Å)	9.66082(19)	17.4231(4)	6.04673(18)
c (Å)	19.0579(4)	10.3673(2)	16.0349(4)
α (°)	90	90	90
β (°)	103.034(2)	92.5434(17)	107.970(4)
γ (°)	90	90	90
V (Å^3)	1612.54(6)	1791.52(6)	1747.40(10)
Z	4	4	4
D_c (g cm^{-3})	1.788	1.744	1.782
μ (Mo K_α) (mm^{-1})	2.040	1.987	2.173
Crystal size (mm)	0.35 × 0.35 × 0.30	0.30 × 0.20 × 0.20	0.30 × 0.20 × 0.20
Crystal shape and color	Colourless prism	Colourless prism	Colourless prism
T_{Min}/T_{Max}	0.448/0.542	0.630/0.671	0.524/0.648
No. data measured	12316	9163	8567
Unique data (R_{int})	2850 (0.0146)	3149 (0.0139)	3077 (0.0112)
Observed data [$I > 2\sigma(I)$]	2677	2824	2905
Final $R1$, $wR2$ (obs. data)	0.0198, 0.0616	0.0210, 0.0507	0.0198, 0.0536
Final $R1$, $wR2$ (all data)	0.0215, 0.0623	0.0255, 0.0519	0.0219, 0.0657
ρ_{max}, ρ_{min} (e Å^{-3})	0.462, −0.223	0.783, −0.194	0.497, −0.416

the CSD regarding compounds involving the Zn-adenine moiety, 22 molecular structures meeting the above-mentioned structural criterion have been deposited in the database. By interpreting these results, it may be concluded that the adenine moiety is coordinated to zinc, depending mainly on a degree of adenine moiety substitution, as a monodentate ligand via the N1-atom [13], N3-atom [14], N7-atom [15] and N9-atom [16], or as a bridging ligand via N1, N7-atoms [17].

The HL_1 ligand is protonated at the N1 position and represents the N1–H protonated N9–H tautomer. The ligand contains three different aromatic rings, i.e. benzene (A), pyrimidine (B) and imidazole (C). Each of these rings deviates slightly from planarity, with the maximum deviations from the mean planes being 0.009(2) Å for the atom C11 (ring A), 0.011(2) Å for the atom C5 (ring B) and 0.0015(19) Å for the atoms C4 and C5 (ring C) [12]. The dihedral angle between the ring A and the purine skeleton (rings B and C) is 80.51(4)°, while the B and C rings are nearly coplanar, with a dihedral angle of 0.98(6)°. Generally, it may be concluded that a degree of deformation within the purine moiety strongly depends on the protonation of the molecule and its coordination mode to a transition metal. Thus, significant changes in interatomic parameters should be noticeable in the vicinity of nitrogen atoms meeting the above-mentioned conditions, mainly in C–N–C angles (see Table 2).

The crystal structure of (**1**) is stabilized by the N–H...Cl, N–H...O, O–H...Cl and N–H...F hydrogen bonds, and C–H...F [C(14)...F(1) = 3.114(3) Å] and C–H...N [C(12)...N(3) = 3.579(2) Å] non-bonding intermolecular interactions. Some of the mentioned contacts are depicted in Figs 2 and 3, while their parameters are summarized in Table 3.

3.1.2. Molecular and crystal structures of $(H_2L_2)[ZnCl_4]\cdot H_2O$ (**2**) and $(H_2L_3)[ZnCl_4]$ (**3**)

The molecular structure of (**2**) together with the atom numbering scheme is depicted in Fig. 4. The structure consists of the twice-protonated H_2L_2 cation, $[ZnCl_4]^{2-}$ anion and one crystal water molecule. The cation exists as the N1–H, N7–H protonated N9–H tautomer and contains benzene (A), pyrimidine (B) and imidazole (C) aromatic rings. Each of these rings deviates slightly from planarity, with the maximum deviations from the mean planes being 0.006(2) Å for the atom C15 (ring A), 0.013(2) Å for the atom C4 (ring B) and 0.007(2) Å for the atom C8 (ring C). The

Table 2
Selected bond lengths (Å) and angles (°) for (**1**), (**2**) and (**3**).

	(**1**)	(**2**)	(**3**)
Bond lengths			
Zn–Cl(1)	2.2414(5)	2.2783(6)	2.2735(6)
Zn–Cl(2)	2.2389(5)	2.2650(5)	2.2754(6)
Zn–Cl(3)	2.2401(5)	2.2564(5)	2.2665(6)
Zn–Cl(4)	–	2.2839(5)	2.2868(5)
Zn–N(7)	2.0708(17)	–	–
N(1)–C(2)	1.365(3)	1.368(3)	1.303(3)
N(1)–C(6)	1.365(3)	1.363(2)	1.368(3)
N(3)–C(2)	1.298(3)	1.299(3)	1.347(3)
N(3)–C(4)	1.354(3)	1.357(3)	1.354(3)
N(7)–C(8)	1.321(3)	1.329(3)	1.318(3)
N(7)–C(5)	1.390(3)	1.381(2)	1.383(3)
N(9)–C(8)	1.346(3)	1.329(3)	1.340(3)
N(9)–C(4)	1.361(3)	1.370(3)	1.357(3)
C(5)–C(6)	1.410(3)	1.411(3)	1.415(3)
Bond angles			
N(7)–Zn–Cl(1)	111.99(5)	–	–
N(7)–Zn–Cl(2)	108.98(5)	–	–
N(7)–Zn–Cl(3)	101.60(5)	–	–
Cl(2)–Zn–Cl(1)	110.51(2)	103.89(2)	109.83(2)
Cl(3)–Zn–Cl(1)	110.77(2)	108.04(2)	115.18(2)
Cl(4)–Zn–Cl(1)	–	114.20(2)	106.05(2)
Cl(3)–Zn–Cl(2)	112.72(2)	114.30(2)	106.69(2)
Cl(4)–Zn–Cl(2)	–	109.43(2)	112.05(2)
Cl(3)–Zn–Cl(4)	–	107.155(19)	107.12(2)
C(8)–N(7)–Zn	114.64(14)	–	–
C(5)–N(7)–Zn	140.27(14)	–	–
C(2)–N(1)–C(6)	123.52(18)	124.13(17)	119.75(19)
C(2)–N(3)–C(4)	112.13(18)	111.71(17)	116.11(18)
C(8)–N(7)–C(5)	104.42(17)	107.68(16)	108.72(18)
C(8)–N(9)–C(4)	107.36(17)	107.90(16)	107.68(17)
N(3)–C(2)–N(1)	125.35(19)	125.50(18)	126.0(2)
N(3)–C(4)–N(9)	126.47(19)	125.61(18)	130.18(19)
N(3)–C(4)–C(5)	127.5(2)	126.97(18)	121.50(19)
N(9)–C(4)–C(5)	106.00(18)	107.41(17)	108.31(19)
C(4)–C(5)–N(7)	109.56(18)	106.87(17)	105.67(18)
C(4)–C(5)–C(6)	117.96(18)	119.74(17)	119.4(2)
N(7)–C(5)–C(6)	132.45(18)	133.33(18)	134.78(19)
N(1)–C(6)–C(5)	113.48(17)	111.90(17)	117.12(18)
N(7)–C(8)–N(9)	112.67(19)	110.13(17)	109.60(19)

Table 3
Hydrogen bonding geometry and intermolecular: and intramolecular interactions for (**1**), (**2**) and (**3**).

D–H...A	*d*(D–H)	*d*(D...A)	*d*(H–A)	<(DHA)
*For (**1**)*				
N(1)–H(1A)...O(1)	0.88	2.772(2)	1.93	159
N(6)–H(6A)...Cl(1)	0.88	3.236(2)	2.36	174
N(9)–H(9C)...F(1)^{i}	0.88	2.895(2)	2.13	144
O(1)–H(1V)...Cl(2)^{ii}	0.88(2)	3.366(2)	2.50(2)	170(3)
O(1)–H(1W)...Cl(1)^{iii}	0.88(2)	3.490(2)	2.61(2)	172(3)
*For (**2**)*				
N(1)–H(1A)...Cl(4)^{iv}	0.88	3.160(2)	2.39	146
N(6)–H(6A)...Cl(2)^{v}	0.88	3.196(2)	2.33	170
N(7)–H(7A)...Cl(2)^{v}	0.88	3.369(2)	2.56	152
N(7)–H(7A)...Cl(1)^{v}	0.88	3.308(2)	2.76	121
N(9)–H(9C)...O1	0.88	2.681(2)	1.81	168
O(1)–H(1 V)...Cl(4)^{vi}	0.892(18)	3.3227(15)	2.50(2)	154(3)
O(1)–H(1 W)...Cl(3)^{vii}	0.878(18)	3.2268(15)	2.39(2)	159(3)
*For (**3**)*				
N(6)–H(3)...Cl(1)	0.88	3.239(2)	2.52	139
N(3)–H(3)...Cl(4)	0.88	3.225(2)	2.61	128
N(3)–H(3)...Cl(3)^{viii}	0.88	3.364(2)	2.95	111
N(6)–H(6A)...Cl(3)^{ix}	0.88	3.208(2)	2.62	126
N(7)–H(7)...Cl(2)^{x}	0.88	3.052(2)	2.28	146
N(7)–H(7)...Cl(3)^{ix}	0.88	3.246(2)	2.73	118
N(9)–H(9)...Cl(4)^{xi}	0.88	3.142(2)	2.52	129
N(9)–H(9)...Cl(4)	0.88	3.245(2)	2.66	125

Symmetry codes: (i) $x-1, -y+1/2, z-1/2$; (ii) $x, -y+1/2, z-1/2$; (iii) $-x+2, y+1/2, -z+3/2$; (iv) $x+1/2, -y+3/2, z+1/2$; (v) $x+1/2, -y+3/2, z-1/2$; (vi) $-x+1, -y+1, -z+1$; (vii) $-x+1/2, y-1/2, -z+1/2$; (viii): $x, y-1, z$; (ix) $x, -y+3/2, z+1/2$; (x) $x, -y+1/2, z+1/2$; (xi) $-x+1, y-1/2, -z+1/2$.

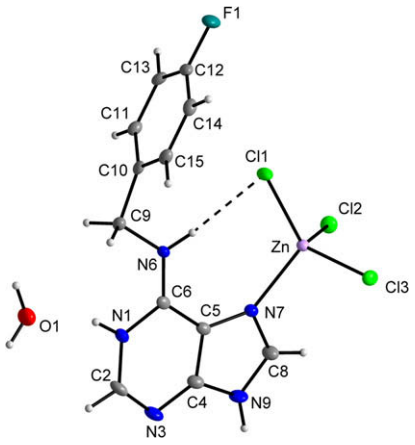

Fig. 1. The molecular structure of complex (**1**), showing the atom numbering scheme. Dashed line indicates the intramolecular N(6)–H...Cl(1) hydrogen bond. Thermal ellipsoids are drawn at the 50% probability level.

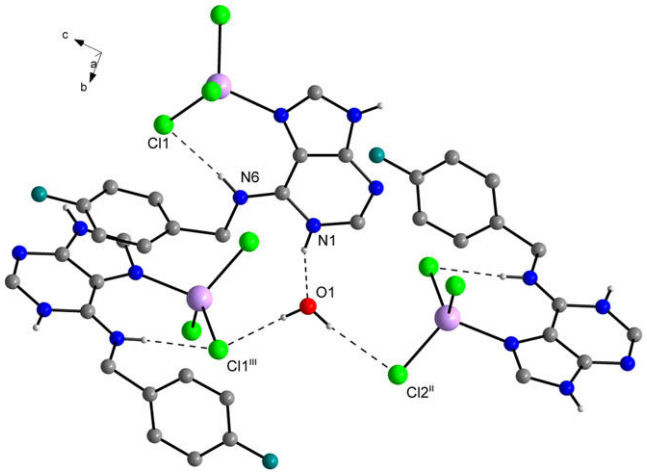

Fig. 2. A part of the crystal structure of (**1**), showing the N–H...Cl, N–H...O and O–H...Cl hydrogen bonds (dashed lines) [Symmetry codes: (ii): $x, \frac{1}{2}-y, -\frac{1}{2}+z$, (iii): $2-x, \frac{1}{2}+y, 3/2-z$]. Some of the H-atoms are omitted for clarity.

dihedral angle between the ring A and the purine skeleton (rings B and C) is 78.39(5)°, while the B and C rings are nearly coplanar, with a dihedral angle of 3.14(7)°. The Zn—Cl bond lengths [2.2564(5)–2.2839(5) Å] are comparable with the average bond length of 2.270(1) Å found in 329 compounds containing a $ZnCl_4$ motive deposited in CSD [7].

The N–H...O and O–H...Cl hydrogen bonds and C...C non-bonding (plane-to-plane distance is ca 3.35 Å) intermolecular contacts contribute to the stabilization of the crystal structure of (**2**). These interactions are depicted in Figs. 5 and 6, while the parameters of hydrogen bonds are summarized in Table 3.

The molecular structure of (**3**) together with the atom numbering scheme is depicted in Fig. 7. Similarly as in the case of (**2**), the structure of (**3**) consists of the twice-protonated H_2L_3 cation and $[ZnCl_4]^{2-}$ anion. The cation exists as the N3–H, N7–H protonated N9–H tautomer and contains benzene (A), pyrimidine (B) and imidazole (C) aromatic rings. Each of these rings deviates slightly from planarity, with the maximum deviations from the mean planes being 0.010(2) Å for the atom C15 (ring A), 0.015(2) Å for the atom C5 (ring B) and 0.008(2) Å for the atom C8 (ring C). The dihedral angle between the ring A and the purine skeleton (rings B and C) is 84.08(5)°, while the B and C rings are nearly coplanar, with a dihedral angle of 2.12(7)° [0.98(6)° in (**1**), 3.14(7)° in (**2**)].

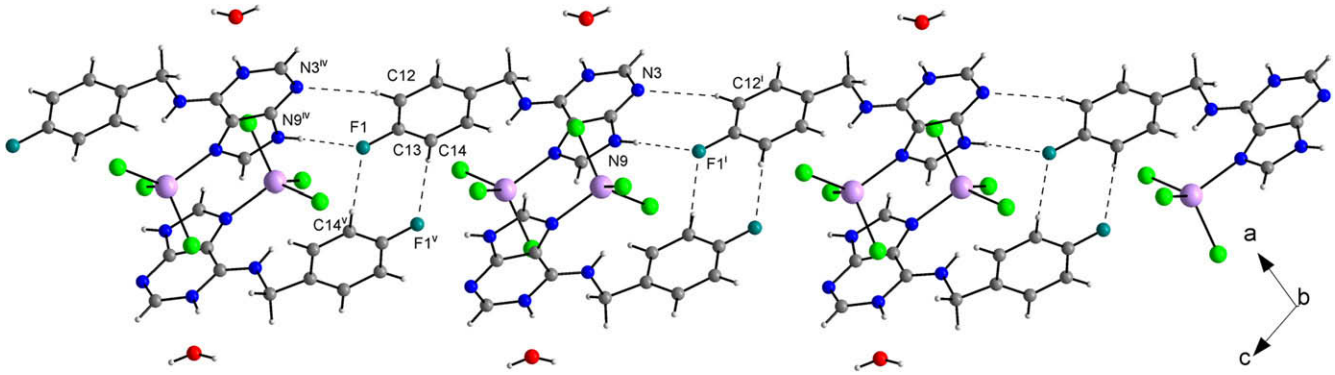

Fig. 3. A part of the crystal structure of (**1**), showing the N–H...F, C–H...F and C–H...N intermolecular contacts (dashed lines) [Symmetry codes: (i): $-1+x$, $\frac{1}{2}-y$, $-\frac{1}{2}+z$, (xii): $1+x$, $\frac{1}{2}-y$, $\frac{1}{2}+z$, (xiii): $2-x$, $1-y$, $2-z$].

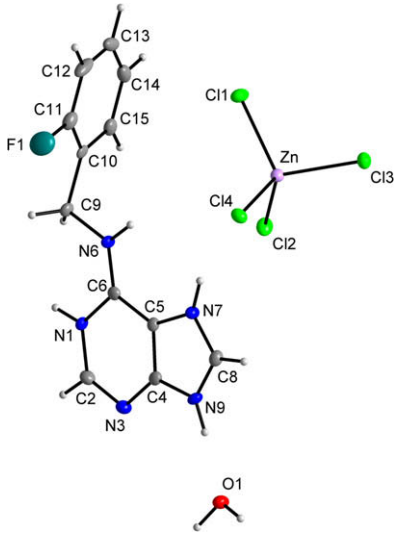

Fig. 4. The molecular structure of complex (**2**), showing the atom numbering scheme. Thermal ellipsoids are drawn at the 50% probability level.

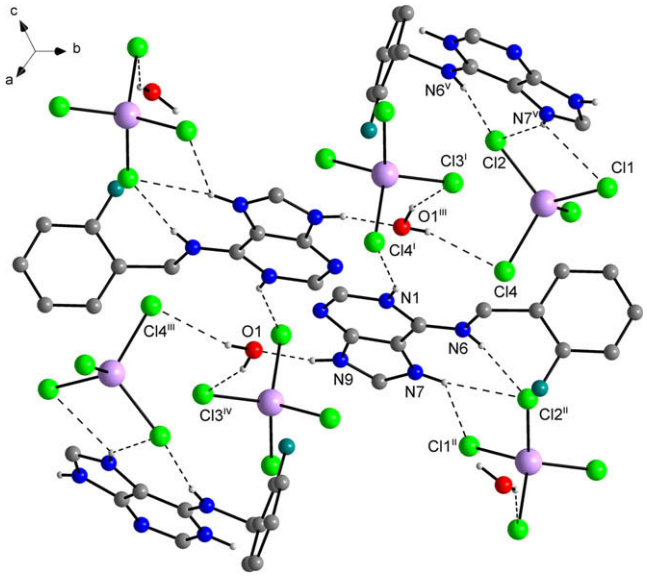

Fig. 5. A part of the crystal structure of (**2**), showing the N–H...Cl, N–H...O and O–H...Cl hydrogen bonds (dashed lines) [Symmetry codes: (iv): $\frac{1}{2}+x$, $\frac{3}{2}-y$, $\frac{1}{2}+z$, (v): $\frac{1}{2}+x$, $\frac{3}{2}-y$, $-\frac{1}{2}+z$, (vi): $1-x$, $1-y$, $1-z$, (vii): $\frac{1}{2}-x$, $-\frac{1}{2}+y$, $\frac{1}{2}-z$, (xiv): $-\frac{1}{2}+x$, $\frac{3}{2}-y$, $\frac{1}{2}+z$]. Most of the H-atoms are omitted for clarity.

The Zn—Cl bond lengths [2.2665(6)–2.2868(5) Å] are comparable with the average bond length of 2.270(1) Å found in compounds containing a $ZnCl_4$ motive deposited in the CSD [7].

The crystal structure of (**3**) is stabilized by the N–H...Cl hydrogen bonds (see Fig. 8) and C...Cl non-bonding intermolecular contacts (see Fig. 9) with the C(2)...Cl(5) separation of 3.252(2) Å. The parameters of the former interactions are summarized in Table 3.

3.2. FTIR and Raman spectra

For the FTIR, Raman and TG/DTA studies, the complex of (**1**) was prepared in a solvated form with the composition of $[Zn(HL_1)Cl_3]\cdot(HL_1Cl)\cdot MeOH$ (**1a**), although the same preparative procedure as described in the Section 2.3.1. was used. FTIR spectra of the compounds (**1a**), (**2**) and (**3**) were measured in the region of 200–4000 cm^{-1}. The spectra clearly confirmed the presence of the organic molecules L_n in the compounds (**1a**), (**2**), and (**3**). The bands observed at 3206–3302 cm^{-1} and 3072–3176 cm^{-1} are assignable to ν(N–H), and $\nu(C–H)_{ar}$, respectively, while very strong bands between 1653 and 1675 cm^{-1} may be attributed to $\nu(C{=}N)_{ar}$ [18]. The ν(C=N) and ν(C=C) purine skeletal vibrations were observed at 1606, 1510, 1447 and 1432 cm^{-1} for (**1a**), 1609, 1588, 1493 and 1454 cm^{-1} for (**2**) and 1625, 1568, 1464 and 1440 cm^{-1} for (**3**). The bands assignable to $\nu(C–F)_{ar}$ were observed at 1223 cm^{-1} for (**1a**) and at 1233 cm^{-1} for (**2**), while the band attributable to $\nu(C–Cl)_{ar}$ was found at 1095 cm^{-1} for (**3**). The values of the last-mentioned maxima are in good accordance with the literature data summarized in the literature [18], where it is claimed that fluorine attached directly to an aromatic ring exhibits a C–F band near 1250 cm^{-1} and a C–Cl band shows maximum between 1000 and 1175 cm^{-1}. Moreover, the measured values correlate well with those of theoretical calculations of vibrational frequencies for 6-(4-fluorobenzylamino)purine, L_1, and 6-(4-chlorobenzylamino)purine, L_3, performed with Spartan06 [19] program package at the B3LYP/6-311+G(d,p) level of theory. The medium strong band calculated at 1239.9 cm^{-1} is connected with the stretching C_{ar}–F vibration, while the maximum belonging to the stretching C_{ar}–Cl vibration was calculated at 1098.3 cm^{-1}. (*Note:* Calculated maxima values were not scaled). Both types of the mentioned vibrations are coupled with the in-plane benzene ring deformation modes. Strong bands at 329 cm^{-1} for (**1a**), 321 cm^{-1} for (**2**) and 313 cm^{-1} for (**3**) are assignable to ν(Zn–Cl), while that at 288 cm^{-1} for (**1a**) may be attributed to ν(Zn–N) [20].

The conclusions supporting the presence of the ligands L_n within the complexes may be also drawn from the Raman spectra. The most intensive bands, which may be assigned to the stretching vibration of the purine skeleton, appeared in the 1337–1345 cm^{-1} region [21]. The vibrations of strong intensity

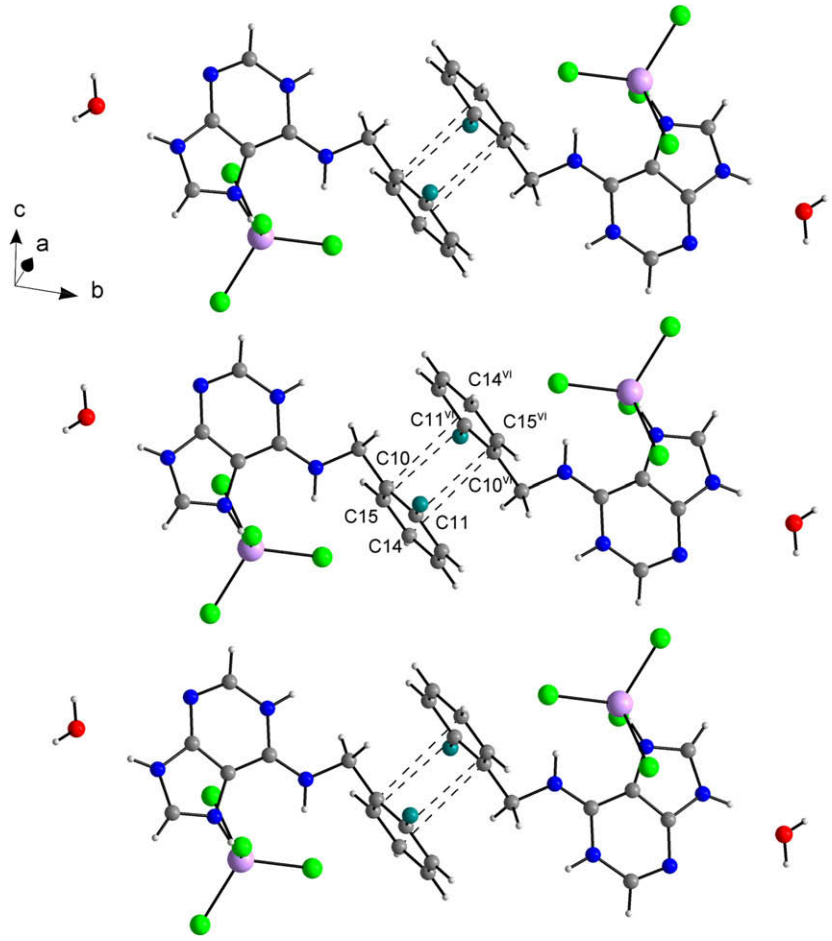

Fig. 6. A part of the crystal structure of (**2**), showing the C. . .C non-bonding contacts (dashed lines) [Symmetry code: (vi): $1-x, 2-y, 1-z$].

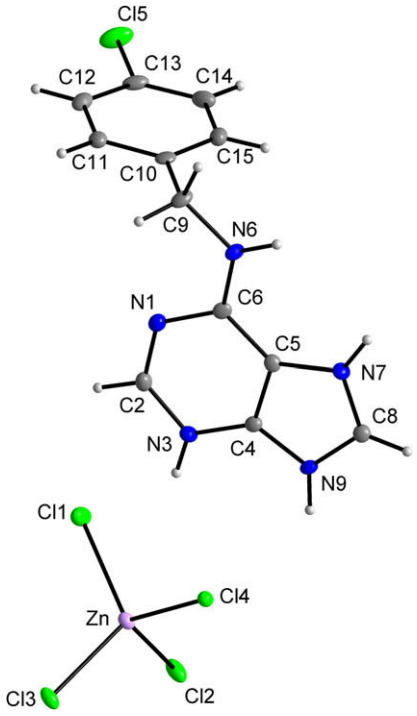

Fig. 7. The molecular structure of complex (**3**), showing the atom numbering scheme. Thermal ellipsoids are drawn at the 50% probability level.

assignable to ν(C=N) were detected at 1605–1623 cm^{-1}. The peaks observed at 278–288 cm^{-1} may be connected with ν(Zn–Cl) vibrations of all compounds, while the peak at 234 cm^{-1} is attributable to ν(Zn–N) in the case of (**1a**) [20].

3.3. Thermal studies

The complexes (**1a**), (**2**) and (**3**) were also studied by means of thermogravimetric (TG) and differential thermal (DTA) analyses. The thermal decomposition of complex (**1a**) is somewhat distinct from those of complexes (**2**) and (**3**) whose decays seem to be nearly identical. The $[Zn(HL_1)Cl_3]\cdot(HL_1Cl)\cdot MeOH$ (**1a**) complex starts to decompose at 96 °C and its thermal decay proceeds in three main steps [see Fig. 10a]. The first weight loss proceeds within the temperature interval of 97–149 °C and is accompanied by a small *endo*-effect on the DTA curve with a minimum at 134 °C. This step may be connected with the elimination of one MeOH molecule of crystallization (a weight loss calcd./found: 4.4/4.8%). The complex exists in the form of $[Zn(HL_1)Cl_3]\cdot(HL_1Cl)$ within the interval of 150–210 °C. Then, the complex decomposes without formation of any thermally stable intermediates up to 638 °C. This part of thermal degradation is accompanied by one small *endo*-effect and three *exo*-effects on the DTA curve with a minimum at 326 °C, and maxima at 342, 443 and 587 °C, respectively. It is supposable that the last-mentioned *endo*-effect cannot be connected with the melting temperature of HL_1Cl molecule of crystallization, i.e. 6-(4-fluorobenzylamino)purine hydrochloride, which was determined to be 213–214 °C, but it may be associated with melting of some Zn-complex intermediate. The thermal decomposition is finished at

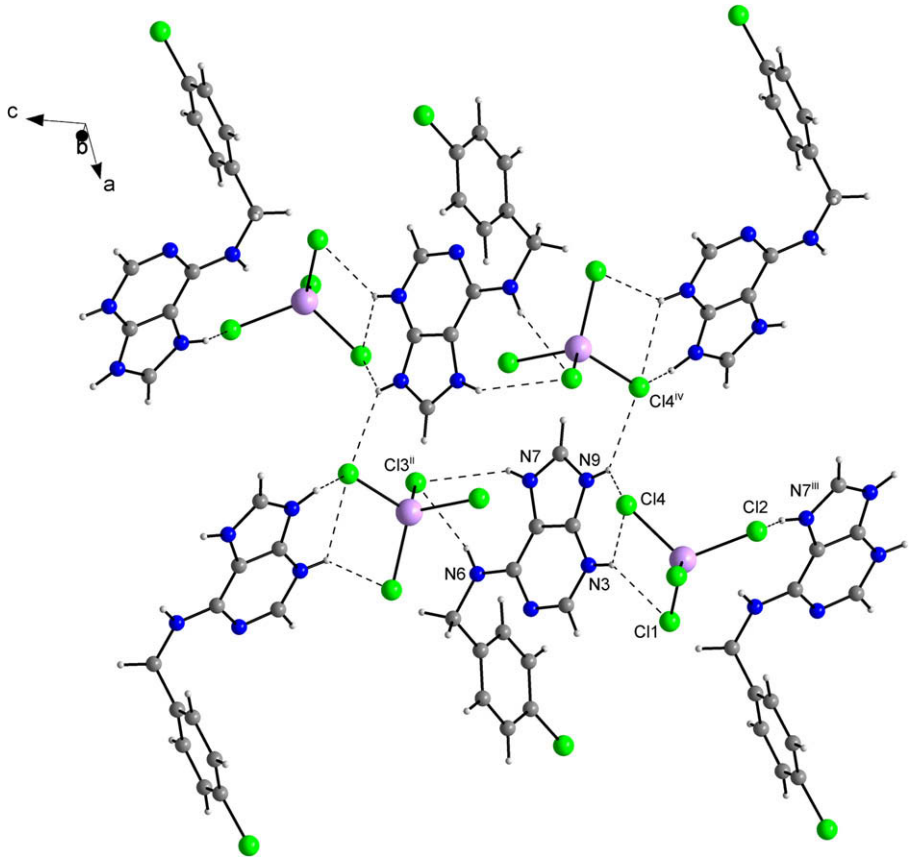

Fig. 8. Part of the crystal structure of (**3**), showing the N–H. . .Cl hydrogen bonds (dashed lines) [Symmetry codes: (ii): *x*, ½ − y, −½ + z, (ix): *x*, 3/2 − *y*, ½ + *z*, (xi): 1 − *x*, −½ + *y*, ½ − *z*].

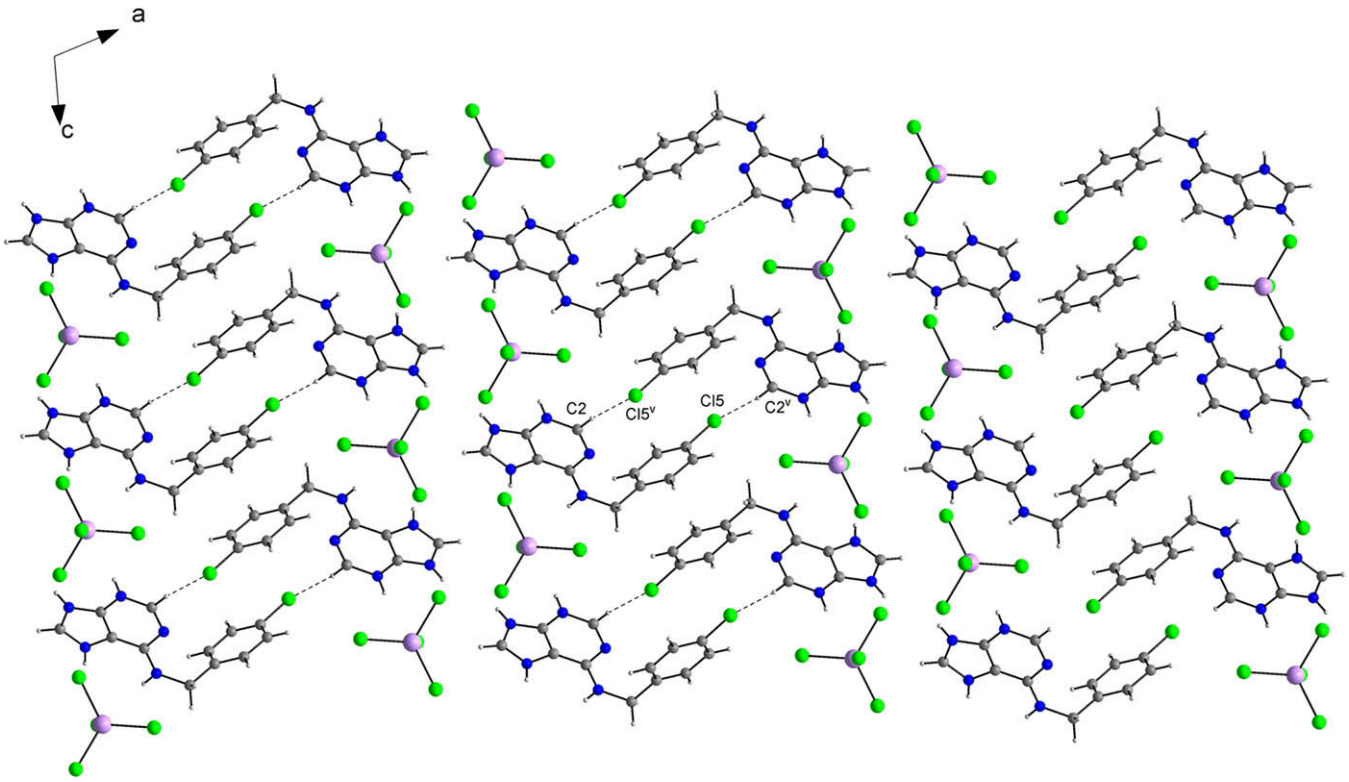

Fig. 9. Part of the crystal structure of (**3**), showing the alternation of cationic and anionic moieties, and C–H. . .Cl non-bonding contacts (dashed lines) [Symmetry code: (v): 2 − *x*, 1 − *y*, 2 − *z*].

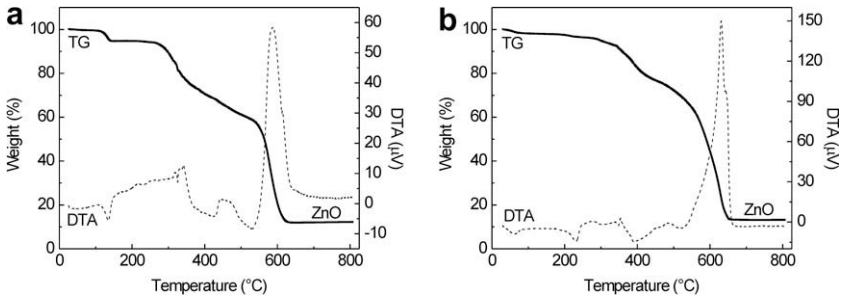

Fig. 10. TG/DTA curves of complexes (**1a**) (*a*) and (**2**) (*b*).

ca 640 °C and is connected with the formation of ZnO as a final product of the degradation (a weight loss calcd./found: 88.8/88.0%).

Based on the fact that the courses of thermal decays of complexes (**2**) and (**3**) are nearly identical, the decomposition of complex (**2**) will be depicted as a representative example [see Fig. 10b]. The complex (**2**) starts to decompose at 33 °C [31 °C for (**3**)]. This first step is accompanied by a small *endo*-effect on the DTA curve with the minimum at 61 °C [53 °C for (**3**)] and can be connected with the elimination of one half of water molecule of crystallization (a weight loss calcd./found: 1.9/2.0%). The unsolvated complex exists between 70 and 200 °C [97–151 °C for (**3**)]. Then, a broad *endo*-effect can be seen on the DTA curve with a minimum at 231 °C [233 °C for (**3**)]. This effect can be connected with the melting and decomposition of the unsolvated complex which is accompanied by a moderate weight loss (1.7%) on the TG curve. This conclusion may be supported by a value of melting temperature of the compound as determined by a melting point apparatus, i.e. 228–230 °C [232–233 °C for (**3**)]. Consequently, the complex decomposes in three steps which are connected with three *exo*-effects with maxima at 354, 470 and 631 °C [350, 443 and 633 °C for (**3**)]. The thermal decomposition is finished at ca 660 °C [690 °C for (**3**)]. ZnO may be considered as a final product of the degradation (a weight loss calcd./found: 88.0/86.8% for **2**).

4. Conclusions

The reactions between $ZnCl_2$ and the 6-benzylaminopurine derivative, L_n, in 0.1 M or 2 M HCl afforded two types of products, i.e. $[Zn(HL_1)Cl_3]\cdot H_2O$ (**1**), and $(H_2L_2)[ZnCl_4]\cdot H_2O$ (**2**) and $(H_2L_3)[ZnCl_4]$ (**3**), in dependence on a pH of the reaction medium. It has been confirmed that the extent of protonation, dominantly depending on the concentration of HCl used, has a significant impact not only on the coordination ability of the discussed organic molecules to Zn(II) cations but also on the changes in interatomic parameters within the variously protonated organic molecules. Moreover, the degree of deformation within the compounds is also markedly influenced by non-bonding intramolecular and intermolecular interactions.

Acknowledgements

The financial support from The Ministry of Education, Youth and Sports of the Czech Republic (a Grant No. MSM6198959218) is gratefully acknowledged. Authors thank Mr. Michal Šipl for help with the preparation of complexes and their single crystals.

Appendix A. Supplementary material

Supplementary data are available from the CCDC, 12 Union Road, Cambridge CB2 1EZ, UK on request, quoting the deposition numbers: CCDC-714074 – CCDC-714076 for (**1**)–(**3**), respectively. Supplementary data associated with this article can be found, in the online version, at doi:10.1016/j.molstruc.2009.06.011.

References

[1] P.J. Davies, Plant Hormones. Biosynthesis, Signal Transduction, Action!, Kluwer Academic Publishers, Dordrecht, The Netherlands, 2004 p. 241.
[2] G. Haberer, J.J. Kieber, Plant. Physiol. 128 (2002) 354.
[3] R.M. Goldsteyn, Cancer Lett. 217 (2005) 129.
[4] F.I. Raynaud, S.R. Whittaker, P.M. Fisher, S. McClue, M.I. Walton, S.E. Barrie, M.D. Garrett, P. Rogers, S.J. Clarke, L.R. Kelland, M. Valenti, L. Brunton, S. Eccles, D.P. Lane, P. Workman, Clin. Cancer Res. 11 (13) (2005) 4875.
[5] Z. Trávníček, A. Klanicová, I. Popa, J. Rolčík, J. Inorg. Biochem. 99 (2005) 776.
[6] Z. Trávníček, L. Szüčová, I. Popa, J. Inorg. Biochem. 101 (2007) 477.
[7] F.H. Allen, Acta Cryst. B58 (2002) 380.
[8] Z. Trávníček, V. Kryštof, M. Šipl, J. Inorg. Biochem. 100 (2006) 214.
[9] J.A. Kuhnle, Physiol. Plant. 41 (1977) 14.
[10] CrysAlis RED and CrysAlis CCD, Version 1.171.32.11, Oxford Diffraction Ltd., Abingdon, England, 2006.
[11] G.M. Sheldrick, Acta Cryst. A64 (2008) 112.
[12] K. Brandenburg, *DIAMOND* (Release 3.1e), Crystal Impact GbR, Bonn, Germany, 2006.
[13] M.J. McCall, M.R. Taylor, Biochim. Biophys. Acta 390 (1976) 137.
[14] M.A. Shipman, C. Price, A.E. Gibson, M.R.J. Elsegood, W. Clegg, A. Houlton, Chem. Eur. J. 6 (2000) 4371.
[15] P. Amo Ochos, P.J.S. Miguel, O. Castillo, M. Sabat, B. Lippert, F. Zamora, J. Biol. Inorg. Chem. 12 (2007) 543.
[16] D. Badura, H. Vahrenkamp, Inorg. Chem. 41 (2002) 6013.
[17] M.J. McCall, M.R. Taylor, Acta Crystallogr. Sect. B Struct. Crystallogr. Cryst. Chem. 32 (1976) 1687.
[18] C.J. Pouchert, The Aldrich Library of Infrared Spectra, third ed., Aldrich Chemical Co., Milwaukee, 1981. pp. 588, 1284.
[19] Spartan06 (Version 1.1.2), Wavefunction Inc. 18401 Von Karman Avenue, Suite 370, Irvine, CA 92612.
[20] K. Nakamoto, Infrared and Raman spectra of inorganic and coordination compounds, Part B: Applications in Coordination, Organometallic, and Bioinorganic Chemistry, fifth ed., Wiley, New York, 1997.
[21] Z. Dhaouadi, M. Ghomi, J.C. Austin, R.B. Girling, R.E. Hester, P. Mojzes, L. Chinsky, P.Y. Turpin, C. Coulombeau, H. Jobic, J. Tomkinson, J. Phys. Chem. 97 (1993) 1074.